Activation of Sirtuin 3 Protects Hippocampal Neurons against Transient Forebrain Ischemic Damage Reducing Oxidative and Inflammatory Responses

In Koo Hwang[1], Kyu Ri Hahn[1], Hyun Jung Kwon[2], Dae Young Yoo[1], Dae Won Kim[2]

[1]*Department of Anatomy and Cell Biology, College of Veterinary Medicine, and Research Institute for Veterinary Science, Seoul National University, Seoul 08826, South Korea*

[2]*Department of Biochemistry and Molecular Biology, Research Institute of Oral Sciences, College of Dentistry, Gangneung-Wonju National University, Gangneung 25457, South Korea*

Introduction

Reactive oxygen species (ROS) are formed by oxidation or reduction or electronic excitation of oxygen molecules and are considered important second-messenger signaling molecules. Under physiological conditions, intracellular ROS concentrations are strictly regulated by antioxidant defense systems, including the glutathione peroxidase and peroxiredoxin/thioredoxin systems. However, ROS concentrations are markedly increased in some pathological conditions; the intracellular antioxidant system does not remove ROS. Ischemia is characterized by oxygen insufficiency or deprivation and suboptimal glucose supply to the brain. This causes marked increments in ROS such as superoxide anions and hydrogen peroxide in mitochondria and results in oxidative stress through the activation of mitochondrial permeability transition pores and mitochondrial dysfunction. Subsequently, ischemia/reperfusion activates inflammatory cascades and causes cellular damage to the brain.

Mongolian gerbils (*Meriones unguiculatus)* are used as animal models for epilepsy, ischemia, cancer, ovarian cysts, the retinal cone system, and Helicobacter pylori. They have an incomplete cerebral arterial circle, and their mortality rate during or after ischemia/reperfusion surgery is relatively low. Recently, genetic engineering techniques involving clustered regularly interspaced short palindromic repeats or their associated proteins have been used to identify therapeutic and protective strategies against ischemic damage. Ischemia/reperfusion injury in gerbils causes neuronal death in some brain regions, including the hippocampus (especially in the CA1 region) 4 days after ischemia. However, ROS release and oxidative damage are detected early (within 6 h) after ischemia/reperfusion without neuronal damage.

Sirtuin 3 (SIRT3), a deacetylase and redox enzyme, controls metabolic transitions during mitochondrial respiration and glycolysis. Glycolytic and related enzymes demonstrate neuroprotective effects against ischemic damage, and the administration of exogenous L-lactate significantly increases SIRT3 expression in the hippocampus.

Sirtuin 3 (SIRT3), a deacetylase and redox enzyme, controls metabolic transitions during mitochondrial respiration and glycolysis. Glycolytic and related enzymes demonstrate neuroprotective effects against ischemic damage, and the administration of exogenous L-lactate significantly increases SIRT3 expression in the hippocampus. Exogenous L-lactate also performs various biological functions through the deacetylation of cyclophilin D and peroxisome proliferator-activated receptor gamma coactivator 1-alpha in the mitochondrial matrix. It decreases cell damage by blocking mitochondrial permeability and transition pore formation and activating mitochondrial biogenesis. In the brain and spinal cord, SIRT3 protects neurons from neurological injury by reducing oxidative stress and inflammatory cascades. Several studies have demonstrated the expression of SIRT3 after neurological diseases, but they have focused on glial expression of SIRT3 and not neurons. In the present study, we examined the chronological and spatial changes in SIRT3 expression in the hippocampal CA1 region and investigated the effects of adjudin, an activator of SIRT3, on ischemic damage in the gerbil hippocampal CA1 region.

Conclusion

The immunoreactivity of SIRT3 was mainly observed in neurons of the stratum pyramidale, and its expression was significantly reduced 2 days after ischemia. SIRT3 immunoreactivity was also observed in glial components after neuronal damage in the CA1 region. The activation of SIRT3 by adjudin treatment ameliorates neuronal damage induced by ischemia/reperfusion via antioxidant and anti-inflammatory pathways. The time window for adjudin treatment remains to be elucidated for its use as a therapeutic agent for transient forebrain ischemia.

Results

1. Changes in SIRT3 expression in the hippocampal CA1 region after ischemia/reperfusion

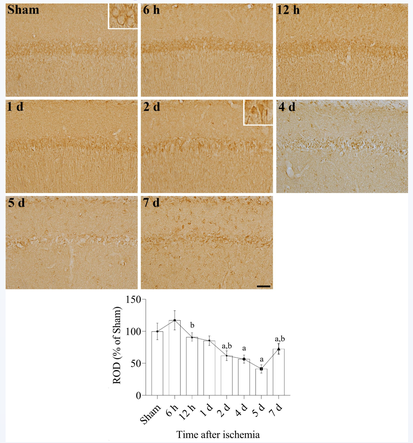

Spatial- and temporal changes in SIRT3 expression in the hippocampal CA1 region after 5 min of transient forebrain ischemia in gerbils. The mid-point of the CA1 region was selected, and SIRT3 immunoreactive structures were quantified based on optical densities and pixel numbers. The data obtained were summed and calibrated into percentile values versus the sham group. The data were analyzed using one-way analysis of variance followed by Tukey's multiple comparison *post hoc* test (n = 5 in the sham group or ischemic group in each time point; $^{a}p < 0.05$, significantly different from the sham group; $^{b}p < 0.05$, significantly different from the pre-adjacent group). The bars indicate the mean values ± standard deviation.

2. Effects of adjudin, a SIRT3 inhibitor, on SIRT3 expression in the CA1 region

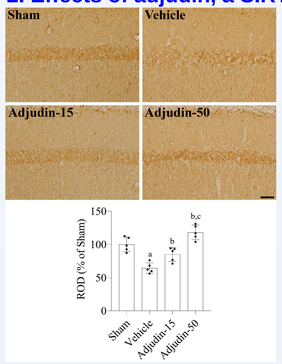

Effects of adjudin treatment on the expression of SIRT3 in the hippocampal CA1 region of sham-operated (Sham), vehicle-treated ischemia-operated (Vehicle), 15 mg/kg adjudin-treated ischemia-operated (Adjudin-15), and 50 mg/kg adjudin-treated ischemia-operated (Adjudin-50) groups 2 days after ischemia/reperfusion. The mid-point of the CA1 region was selected, and SIRT3 immunoreactive structures were quantified based on optical densities and pixel numbers. The data obtained were summed and calibrated into percentile values versus the sham group. The data were analyzed using one-way analysis of variance followed by Tukey's multiple comparison *post-hoc* test (n = 5; $^{a}p < 0.05$, significantly different from the Sham; $^{b}p < 0.05$, significantly different from the Vehicle; $^{c}p < 0.05$, significantly different from the Adjudin-15). The bars indicate the mean values ± standard deviation.

3. Effects of adjudin on spontaneous motor activity and neuronal damage

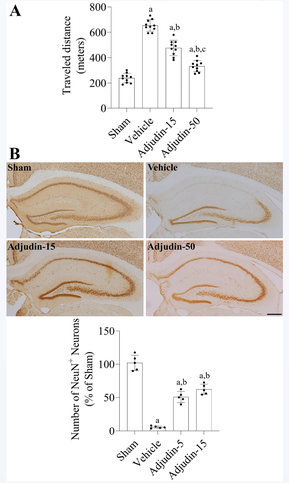

Effects of adjudin treatment on the locomotor activity and neuronal damage in the hippocampus of sham-operated (Sham), vehicle-treated ischemia-operated (Vehicle), 15 mg/kg adjudin-treated ischemia-operated (Adjudin-15), and 50 mg/kg adjudin-treated ischemia-operated (Adjudin-50) groups 1 and 4 d after ischemia/reperfusion, respectively. (A) The movement of gerbils was recorded, and the distance traveled was analyzed at 24 h after ischemia. (B) NeuN immunohistochemical staining was conducted to detect the surviving neurons in the hippocampus 4 days after ischemia. Scale bar = 400 μm. NeuN immunoreactive structures located in the mid-point of the CA1 region were selected, and the optical densities were quantified based on optical densities and pixel numbers. The data obtained were summed and calibrated into percentile values versus the sham group. The data were analyzed using one-way analysis of variance followed by Tukey's multiple comparison *post hoc* test (n = 10 for locomotor activity or 5 for NeuN immunohistochemistry; $^{a}p < 0.05$, significantly different from the Sham; $^{b}p < 0.05$, significantly different from the Vehicle; $^{c}p < 0.05$, significantly different from the Adjudin-15). The bars indicate the mean values ± standard deviation.

4. Effects of adjudin on microglial activation and proinflammatory cytokine release

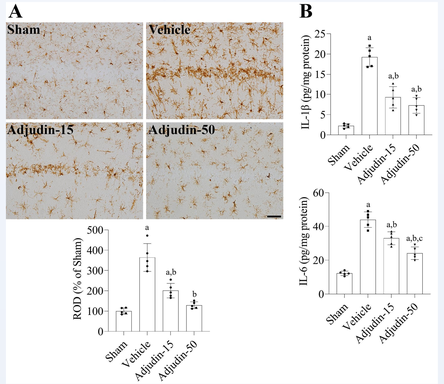

Effects of adjudin treatment on the morphology of Iba1 immunoreactive microglia and pro-inflammatory cytokine releases of sham-operated (Sham), vehicle-treated ischemia-operated (Vehicle), 15 mg/kg adjudin-treated ischemia-operated (Adjudin-15), and 50 mg/kg adjudin-treated ischemia-operated (Adjudin-50) groups at 4 d and 6 h after ischemia/reperfusion, respectively. (A) Iba1 immunoreactive microglia was visualized in the CA1 region 4 d after ischemia. The mid-point of the CA1 region was selected, and Iba1 immunoreactive structures were quantified based on optical densities and pixel numbers. The data obtained were summed and calibrated into percentile values versus the sham group. (B) Pro-inflammatory cytokines such as IL-1β and IL-6 were quantified in the hippocampal homogenates 6 h after ischemia/reperfusion. (A and B) The data were analyzed using one-way analysis of variance followed by Tukey's multiple comparison *post hoc* test (n = 5; $^{a}p < 0.05$, significantly different from the Sham; $^{b}p < 0.05$, significantly different from the Vehicle; $^{c}p < 0.05$, significantly different from the Adjudin-15). The bars indicate the mean values ± standard deviation.

5. Effects of adjudin on ROS formation and GPx concentration

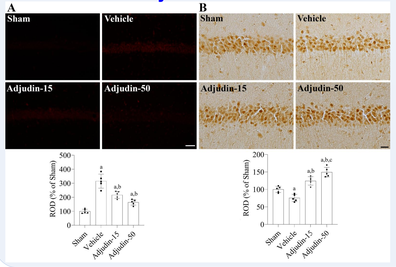

Effects of adjudin treatment on ROS formation and GPx expression in the hippocampal CA1 region of sham-operated (Sham), vehicle-treated ischemia-operated (Vehicle), 15 mg/kg adjudin-treated ischemia-operated (Adjudin-15), and 50 mg/kg adjudin-treated ischemia-operated (Adjudin-50) groups at 3 h and 2 d after ischemia/reperfusion, respectively. (A) ROS formation was visualized by histochemical staining using DHE in the hippocampus 3 h after ischemia/reperfusion. (B) GPx immunohistochemical staining was performed in the hippocampal CA1 region 2 d after ischemia/reperfusion. (A and B) The mid-point of the CA1 region was selected, and DHE fluorescent and GPx immunoreactive structures were quantified based on optical densities and pixel numbers. The data obtained were summed and calibrated into percentile values versus the sham group. Data are analyzed using one-way analysis of variance followed by Tukey's multiple comparison *post hoc* test (n = 5; $^{a}p < 0.05$, significantly different from the Sham; $^{b}p < 0.05$, significantly different from the Vehicle; $^{c}p < 0.05$, significantly different from the Adjudin-15). The bars indicate the mean values ± SD